Hindawi
Journal of Probability and Statistics
Volume 2022, Article ID 4170866, 19 pages
https://doi.org/10.1155/2022/4170866

Research Article

Nonstationary Generalised Autoregressive Conditional Heteroskedasticity Modelling for Fitting Higher Order Moments of Financial Series within Moving Time Windows

Luke De Clerk and Sergey Savel'ev

Department of Physics, Loughborough University, Leicestershire LE11 3TU, UK

Correspondence should be addressed to Luke De Clerk; l.de-clerk@lboro.ac.uk

Received 14 January 2022; Revised 2 March 2022; Accepted 13 April 2022; Published 20 May 2022

Academic Editor: Zacharias Psaradakis

Here, we present a method for a simple GARCH (1,1) model to fit higher order moments for different companies' stock prices. When we assume a Gaussian conditional distribution, we fail to capture any empirical data when fitting the first three even moments of financial time series. We show instead that a mixture of normal distributions is needed to better capture the higher order moments of the data. To demonstrate this point, we construct regions (parameter diagrams), in the fourth- and sixth-order standardised moment space, where a GARCH (1,1) model can be used to fit moment values and compare them with the corresponding moments from empirical data for different sectors of the economy. We found that the ability of the GARCH model with a double normal conditional distribution to fit higher order moments is dictated by the time window our data spans. We can only fit data collected within specific time window lengths and only with certain parameters of the conditional double Gaussian distribution. In order to incorporate the nonstationarity of financial series, we assume that the parameters of the GARCH model can have time dependence. Furthermore, using the method developed here, we investigate the effect of the COVID-19 pandemic has upon stock's stability and how this compares with the 2008 financial crash.

1. Introduction

Modelling of financial time series is a very extensive area of research. One notable breakthrough in financial modelling is the discovery of the heteroskedasticity and conditional nature of volatility, manifesting itself in a slow stochastic process in the dynamics of price variance, in addition to the fast fluctuating price process itself. This motivates the development of the Autoregressive Conditional Heteroskedasticity models (ARCH) [1], which was later generalised (GARCH) [2]. The autoregressive processes allow a stochastic model to predict the price change probability density for a given time series. The level of return at a certain instance is described by a probability distribution (usually Gaussian) and the variance of the process. The variance of the process varies with time and is defined by both the variance and level of return at the previous time instance (s). However, GARCH is not limited to simply financial systems but to any system where this two scale stochastic processes is seen, for instance the study by Kumar et al. on atmospheric cycles in [3] or the study on pathogen growth by Ali in [4].

Extensive research has been undertaken to adapt the original Bollerslev GARCH model to fit empirical observations of time series [5–14]. Nevertheless, whilst these modifications of GARCH increase the accuracy of forecasting volatility, there is an increase in the complexity of the models and in the ambiguity of estimating model parameters. For example, fitting higher order statistical moments of financial series is an attractive approach for estimating model parameters [15, 16]. The original GARCH model allows us to obtain analytical relations between the statistical moments and the GARCH model parameters. In contrast, the modifications of the GARCH model lead to an increase in the complexity of the expressions for the higher order

moments making the evaluation of the model parameters very challenging. Therefore, we wish to seek how effective the original GARCH model is at fitting higher order moments of empirical financial data series for different sectors of the economy. The focus of the study upon higher order moments is primarily due to the higher order moments' ability to capture general aspects of a given distribution. It is well documented [17–20] that higher order moments are able to quantitatively represent the number of events that differ largely from the mean value of the process. In essence, they provide a different way to capture and effectively describe the statistical dynamics of the system.

There are several commonly used ways to estimate GARCH parameters [21, 22]. The most relevant and widely used is the Maximum Likelihood Estimation (MLE) [23, 24]. However, there are several pitfalls of such a task, the main one is the assumption of statistical properties within the empirical data. If this assumption is wrong, the estimated parameters are not reliable. Consequently, there has been significant work to adapt and implement the generalised method of moments (GMM) to the realm of financial studies [15, 16]. We can set a task to fit a certain set of statistical moments, for example $\langle x^2 \rangle$, $\langle x^4 \rangle$, and $\langle x^6 \rangle$. As we have three parameters of the GARCH (1,1) model, we can solve this task using relations between the higher order moments and GARCH parameters derived in [2], and so we can undertake a GMM algorithm for a GARCH (1,1) model. We can ask if we can or cannot fit three empirically estimated moments of a chosen stock price series by three GARCH (1,1) parameters. The region where the parameters of the GARCH model can fit empirical moments shall be referred to throughout as the GARCH existence region or the "GARCHable" region. If we evaluate the time series and conclude that GARCH (1,1) parameters cannot fit empirical moments, then we can judge that the time series might no longer be purely stationary or a significant modification of the GARCH (1,1) model is needed to capture the dynamics.

As in the case of stocks and shares, the global economic climate and external factors are major stressors when determining the price of a given stock. Such a complex dependence of factors leads to a very fluid economic environment. Higher order moment analysis can determine the behaviour of the time series in response to this economic environment. However, economic factors affect the individual time series on different time scales. As such, the time window we analyse for the financial series will show different signatures for these different time scales as well as economic cycles and general tendencies. Therefore, it is plausible that truncating the time series into different time windows, we will gain different sets of model parameters for each time interval. The information about the changing behaviour of time series can manifest itself in a variation of the GARCH parameters and can identify changing economic factors and trends, including crisis periods [25]. The idea of truncating empirical data to relatively short time windows can be challenged by the necessity to have long data sampling to accurately estimate higher order statistical moments, especially, if the moment values significantly exceed the corresponding Gaussian values. This motivates us to develop a practical procedure by combining empirical studies of higher order moments within medium to long time windows with reasonable accumulated statistics and evaluating GARCH parameters from asymptotic analytical expressions of higher order moments derived in [2]. In this study, we analysed data for the period of 6 October 2000 to 6 October 2018, in most cases we use a subset of this data set. For example, this can be divided into a pre-crisis, post-crisis, and crisis period. This division is extremely valuable in deducing the statistical features that are inherent to an economic crisis. This will be reflected in the results we gain from evaluating certain statistical moments in the years from 2000 to 2018.

The study is organised as follows: in Section 2, we initially analyse the sixth-order moment for several companies and discuss the economic environments. In Appendix E, we present the findings for quarterly truncated time windows. In Section 3, we discuss the methods we will be using and how we have created the parameter diagrams in higher order moment space where GARCH can describe empirical data. Section 4 presents our findings for a GARCH model with a Gaussian conditional probability distribution (we will proceed calling these GARCH-normal models) for empirical time-series fitting, whilst also showing the failure of the GARCH-normal models to describe higher order moments of financial time series. In Section 5, we discuss a GARCH model with a double Gaussian conditional probability distribution (GARCH-double-normal models) to account for this shortfall. We also show how with the assumption of time-dependent parameters, the data we analyse can be described by nonstationary GARCH-double-normal models. In Section 6, we discuss problems faced when using the likelihood method for an empirical data set, with given fourth- and sixth-order standardised moments. In Section 7, we perform analysis upon data series from the COVID-19 pandemic crisis period. Finally, Section 8 concludes our study.

2. Raw Data Analysis

In order to determine the behaviour of the moments of financial time series, we first highlight the time dependence of the sixth-order moment for several companies and a government bond (gilt) through the financial crisis of 2008. To do this, we use the daily closing price of each trading day over 6 month periods for 8 years, 2002–2010. We then use the following equation to calculate the nth-order moment:

$$\langle x^n \rangle (t) = \frac{1}{N} \sum_{t-(N/2)\delta t < \tau < t+(N/2\delta t} \left(x(\tau) - \frac{1}{N} \sum_{t-(N/2)<\tau_1<t+(N/2)} x(\tau_1) \right)^n, \quad (1)$$

where we take N to be 6 months, so the period we average over is 126 days (due to trading exclusion dates) and each time step δt a trading day. Here, we define x as the logarithm of price change:

$$x(\tau) = \ln\left(\frac{y(\tau + \delta t)}{y(\tau)}\right), \tag{2}$$

$y(\tau)$ is the closing price at day τ. In this study, we also consider the average over a longer time history, for example when $M = 4536$, in essence, we consider an 18-year time horizon:

$$\langle x^n \rangle = \frac{1}{M}\sum_{i=1}^{M}\left(x(t_0 + i\delta t) - \frac{1}{M}\sum_{j=1}^{M} x(t_0 + j\delta t)\right)^n, \tag{3}$$

where t_0 corresponds to 6th October 2000. We also evaluate empirical standardised moments for higher order moments:

$$\Gamma_{2m} = \frac{\langle x^{2m} \rangle}{\langle x^2 \rangle^m}. \tag{4}$$

Figure 1 shows the behaviour of the sixth-order statistical moment in response to a shifting time window. To create the plot, we take an 18-year time series, 2000–2018, and move a six-month long window from the start to finish, with nonoverlapping segments. We then calculate the maximum and minimum values of our error intervals, as described in Appendix A. For the time series between 2000 and 2007, we see a flat response of the higher order moment with respect to time. However, when we move the window over the 2008 financial crash, we see a large increase in the value of the sixth-order moment.

We undertake this analysis for four banking securities and one commodity. For the banking stocks, we can see the value of the sixth-order moment increases within the region of the financial crisis and then once the crisis is over, we see the value of the moment return to this pre-crisis level. The behaviour is not seen in the commodity security, Gold ETFs. What we instead see, is a small increase throughout the financial crisis period, a small deviation from its level before. However, we do see a slight change in the behaviour of the moment of the security before the financial crash, perhaps a pre-cursor to the turmoil to come. It can thus be seen from this simple analysis, that the banking securities have a very distinct behaviour.

3. Stochastic Model

In this section, we focus upon a GARCH-normal (1,1) model. We can see from Bollerslev's work [2] that for such a model x_t is a random variable with zero mean and possesses the conditional variance, σ_t^2. We define $x_t \equiv \zeta_t \sigma_t$. Here, ζ_t is a random process with zero mean and variance equal to one. Depending on the system, we wish to model the variable ζ_t can be described by different probability distributions, see for example [8, 26–29]. Following [17], we first assume the conditional probability to be Gaussian, we will refer to such models as the GARCH-normal model. The GARCH (1,1) processes are defined via the relation:

$$\sigma_t^2 = \alpha_0 + \alpha_1 x_{t-1}^2 + \beta_1 \sigma_{t-1}^2, \tag{5}$$

where, α_0, α_1, and β_1 are the parameters, whilst $t - 1$ refers to the previous value of the conditional variance and the previous value of the innovation x_t. If we know the exact probability density $p(x)$ of a process, we could write the definition of moments by $E[x^m] = \int_{-\infty}^{\infty} P(x) x^m \mathrm{d}x$. However, we do not know the analytical expression for the probability distribution of the GARCH process. To resolve this problem, Bollerslev [2] proposed the recurrence relations for moments of the GARCH-normal (1,1) model:

$$E\left(x_t^{2m}\right) = \frac{a_m\left[\sum_{n=0}^{m-1} a_n^{-1}\left(E\left(x_t^{2n}\right)\right)\alpha_0^{m-n}\binom{m}{m-n}\mu(\alpha_1, \beta_1, n)\right]}{[1 - \mu(\alpha_1, \beta_1, m)]}, \tag{6}$$

where

$$\mu(\alpha_1, \beta_1, m) = \sum_{j=0}^{m}\binom{m}{j} a_i \alpha_1^j \beta_1^{m-j}, a_j = \prod_{i=1}^{j}(2i - 1). \tag{7}$$

Therefore, we can derive equations for the unconditional variance, the fourth-order and sixth-order standardised moments [17]:

$$\sigma^2 = \frac{\alpha_0}{1 - \alpha_1 - \beta_1}, \tag{8}$$

$$\Gamma_4 = \frac{E\left(x_t^4\right)}{E\left(x_t^2\right)^2} = 3 + \frac{6\alpha_1^2}{1 - 3\alpha_1^2 - 2\alpha_1\beta_1 - \beta_1^2}, \tag{9}$$

$$\Gamma_6 = \frac{E\left(x_t^6\right)}{\left(E\left(x_t^2\right)\right)^3} = \frac{15(1 - \alpha_1 - \beta_1)^3\left(1 + (3(\alpha_1 + \beta_1)/1 - \alpha_1 - \beta_1) + \left(3\left(1 + (2(\alpha_1 + \beta_1)/1 - \alpha_1 - \beta_1)\right)\left(\beta_1^2 + 2\alpha_1\beta_1 + 3\alpha_1^2\right)/1 - 3\alpha_1^2 - 2\alpha_1\beta_1 - \beta_1^2\right)\right)}{1 - 15\alpha_1^3 - 9\alpha_1^2\beta_1 - 3\alpha_1\beta_1^2 - \beta_1^3}. \tag{10}$$

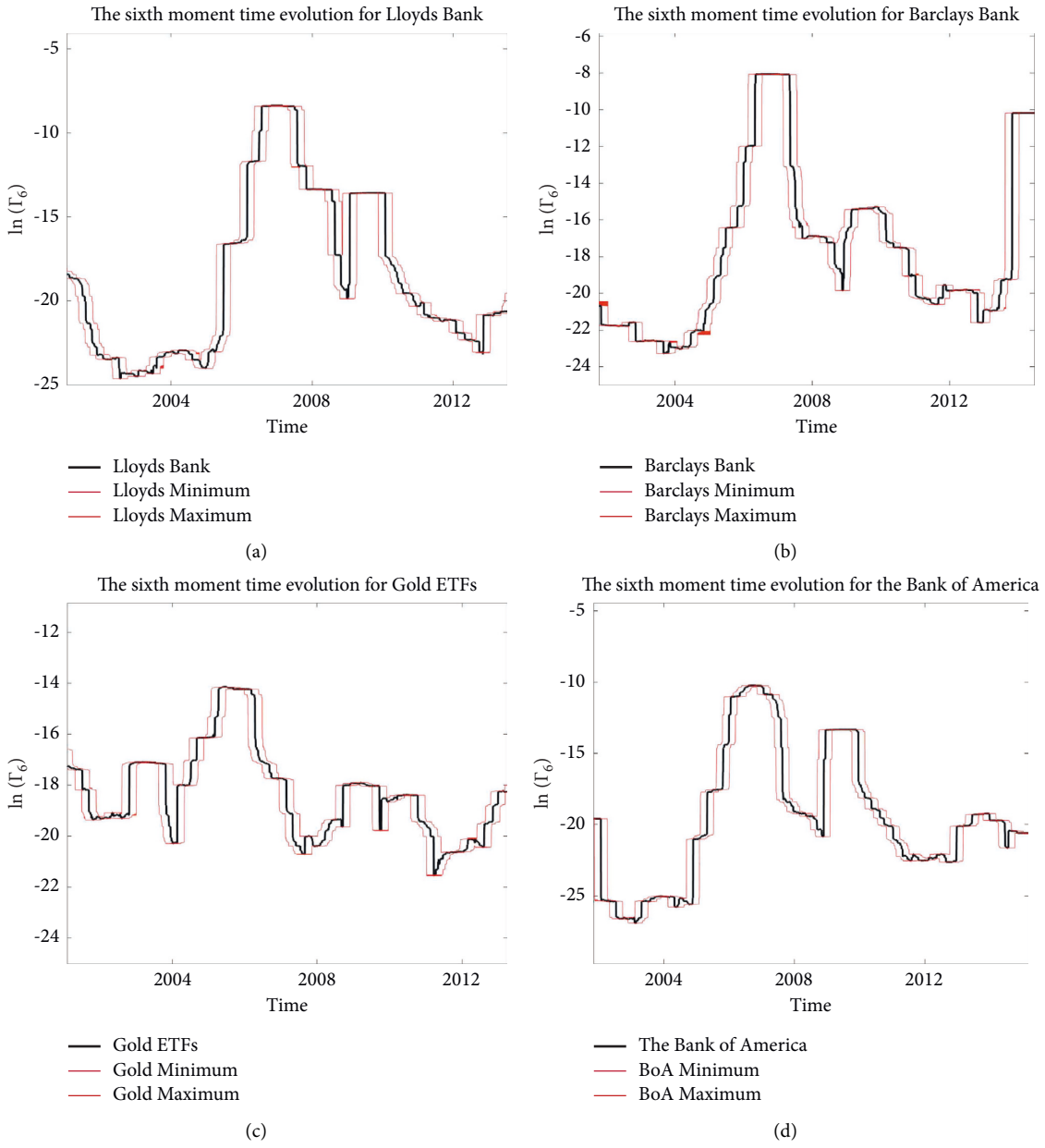

FIGURE 1: The behaviour of the logarithm of the sixth-order moment for six-month long intervals from 2000 to 2018, complete with the error intervals, shown by the solid red lines for each security, for details see A. During the crisis period, 2007–2009, we see a spike in the value of the raw moment for all securities apart from gold. Before and after the financial crisis we see small fluctuations in the value of the sixth-order moment over time. (a) Lloyds Bank, (b) Barclays Bank, (c) Gold, and (d) the Bank of America.

The relation (6) and (7) define all moments if we fix the three GARCH parameters, α_0, α_1, and β_1. For a moment to exist, we should have $\mu(\alpha_1, \beta_1, m) < 1$. Solving $\mu(\alpha_1, \beta_1, m) = 1$, we obtain the functions $\beta_1 = \beta_1^{(m)}(\alpha_1)$. In doing so, we can create Figure 2 [2]. In this figure, we see the different curves of $\beta_1 = \beta_1^{(m)}(\alpha_1)$ where m takes the value: 2, 4, 6, 8, 10, and 12. When $\beta_1 < \beta_1^{(m)}(\alpha_1)$ the corresponding moments $E[x_t^{2m}]$ and standardised moments Γ_{2m} have finite values, whilst for $\beta_1 > \beta_1^{(m)}(\alpha_1)$, these moments diverge. Since the particular lines $\beta_1 = \beta_1^{(m)}(\alpha_1)$, below called divergence lines, separate the region of parameters where the $2m$-th moment exists and where it does not, we can interpret this as a parameter diagram in model parameter space, [2]. For the second-, fourth-, and sixth-order divergence lines, we are able to gain analytical expressions for the divergence lines, see Appendix B. In Figure 2, we present a filled area that shows the region of existence of the sixth-order moment. The red circle in this figure represents a set of parameter values that allow for the existence of the second, fourth, and sixth moments but not the eighth or higher, while for the black square in Figure 2, only the second- and fourth-order moments are finite.

Whilst the present problem of finding the GARCH moments knowing the three model parameters is

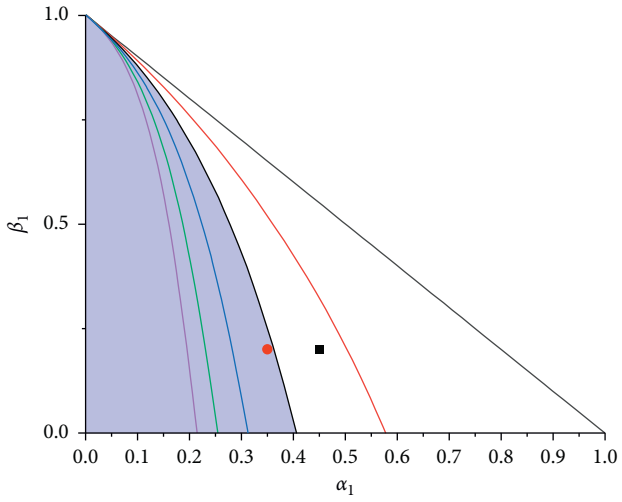

FIGURE 2: The phase diagram, obtained in [2], shows the line of divergence of moments in a GARCH-normal (1,1) model. The highlighted area shows the existence region for the sixth-order moment. The red circle presents an example of α_1, β_1 values that allow for the second-, fourth-, and sixth-order moments to exist, whilst the black square shows an example of α_1, β_1 values that allow for only the second- and fourth-order moments to exist.

straightforward, the inverse problem to estimate the three GARCH parameters, if three moments are known, is much more complicated and reduces to a set of transcendental equations which are hard to solve.

4. GARCH-Normal Models

4.1. Company Trajectories. Here, we will consider the situation of when we need to fit only the second- and fourth-order moments, or equivalently, fitting the unconditional variance $\langle x^2 \rangle$ and fourth-order standardised moment Γ_4. Since the GARCH-normal (1,1) model has three parameters, we can conclude that we can express two GARCH parameters, for instance, α_1 and β_1, as a function of the third parameter α_0. To do so, we use equations (8) and (9) to fit the empirical values of variance σ^2_{emp} and the fourth-order standardised moment, $\Gamma_{4,\text{emp}}$, for a certain company, such that $\sigma^2(\alpha_0, \alpha_1, \beta_1) = \sigma^2_{\text{emp}}$ and $\Gamma_4(\alpha_1, \beta_1) = \Gamma_{4,\text{emp}}$. In doing so, we derive:

$$\alpha_1 = \sqrt{\frac{\left(2\alpha_0/\sigma^2_{\text{emp}}\right) - \left(\alpha_0^2/\left(\sigma^2_{\text{emp}}\right)^2\right)}{\left(6/\Gamma_{4,\text{emp}} - 3\right) + 2}}, \tag{11}$$

$$\beta_1 = \frac{\alpha_0}{\sigma^2_{\text{emp}}} - \sqrt{\frac{\left(2\alpha_0/\sigma^2_{\text{emp}}\right) - \left(\alpha_0^2/\left(\sigma^2_{\text{emp}}\right)^2\right)}{\left(6/\Gamma_{4,\text{emp}} - 3\right) + 2}}. \tag{12}$$

It is clear from these equations that for any value of $\Gamma_{4,\text{emp}} > 3$ and $\sigma^2_{\text{emp}} > 0$, we can find a family of one-parametric GARCH models, corresponding to different values of α_0. So, we obtain the parametric curves; $(\alpha_1(\alpha_0), \beta_1(\alpha_0))$ in (α_1, β_1) space. Such curves represent the "company trajectories" with already fixed (empirical) variance σ^2_{emp} and empirical fourth-order standardised moments $\Gamma_{4,\text{emp}}$.

In Figure 3, we see an extension of Figure 2 for a banking stock, a commodity, a pharmaceutical, and a mining company, respectively. The dotted lines represent the parameters of the GARCH-normal model for the given company's trajectory. They allow us to see the "stability" of the time series, in essence, which statistical moments can exist for the GARCH description of the empirical data of a certain company. It is evident, for the longest time period (18 years) that apart from the gold ETFs (Exchange Traded Funds), trajectories of all other companies lie above the divergence line of the sixth-order moment. This implies that the empirical values of the second- and fourth-order empirical statistical moments do not allow for any higher order moments to be fitted via a GARCH-normal model.

If we decrease the time window of data collection, for example a year, 6 October 2000 to 6 October 2001, or even six months, 6 October 2000 to 6 April 2001, then we can see the migration of the company's trajectory to deeper inside the stability region in the (α_1, β_1) plane, where higher moments are finite (see Figures 3(a)–3(d)). We have also examined the time windows of nine months, fifteen months, and three years. In these figures (Figures 3(a)–3(d)), it is clear that the Rio Tinto 6-month time series allows the largest number of higher order moments to exist for its description within the corresponding GARCH-normal (1,1) model. In general, the shorter a time series we take, the more moments exist for a GARCH-normal (1,1) model.

As we traverse a company's trajectories in (α_1, β_1) space, we can work out the value of the sixth-order standardised moment generated from the GARCH-normal (1,1) model for these specific α_1 and β_1 values. In Table 1, we see the minimum and maximum of Γ_6 which can be achieved. We can see that Γ_6 does not vary significantly along the company's trajectory, resulting in a problem to fit diverse values of the empirical sixth-order standardised moments.

4.2. Methods of Parameter Fitting. If we want to fit the second, fourth, and sixth moments, the values of the parameters must be below the divergence curve: $\beta_1 < \beta_1^{(6)}(\alpha_1)$, which does not cover all parameter space for the existence of the fourth $(\beta_1 < \beta_1^{(4)})$ and second $(\beta_1 < \beta_1^{(2)})$ order moments. This can result in some values of the fourth and second moments, or fourth-order standardised moment and the second-order moment being unreachable for GARCH modelling, see Appendix C.

Let us consider the algorithms we can use to fit empirical values of $\langle x^2 \rangle$, $\langle x^4 \rangle$ and $\langle x^6 \rangle$ which can be reformulated in terms of the variance σ^2_{emp} as well as the fourth- and sixth-order standardised moments $\Gamma_{4,\text{emp}}$ and $\Gamma_{6,\text{emp}}$, respectively. In the first approach, we present α_1 and β_1 as a function of α_0, that is, $\alpha_1(\alpha_0, \sigma^2_{\text{emp}}, \Gamma_{4,\text{emp}})$ and $\beta_1(\alpha_0, \sigma^2_{\text{emp}}, \Gamma_{4,\text{emp}})$, from equations (11) and (12), then numerically solve the equation:

$$\Gamma_6\left(\alpha_1\left(\alpha_0, \sigma^2_{\text{emp}}, \Gamma_{4,\text{emp}}\right), \beta_1\left(\alpha_0, \sigma^2_{\text{emp}}, \Gamma_{4,\text{emp}}\right), \alpha_0\right) = \Gamma_{6,\text{emp}}, \tag{13}$$

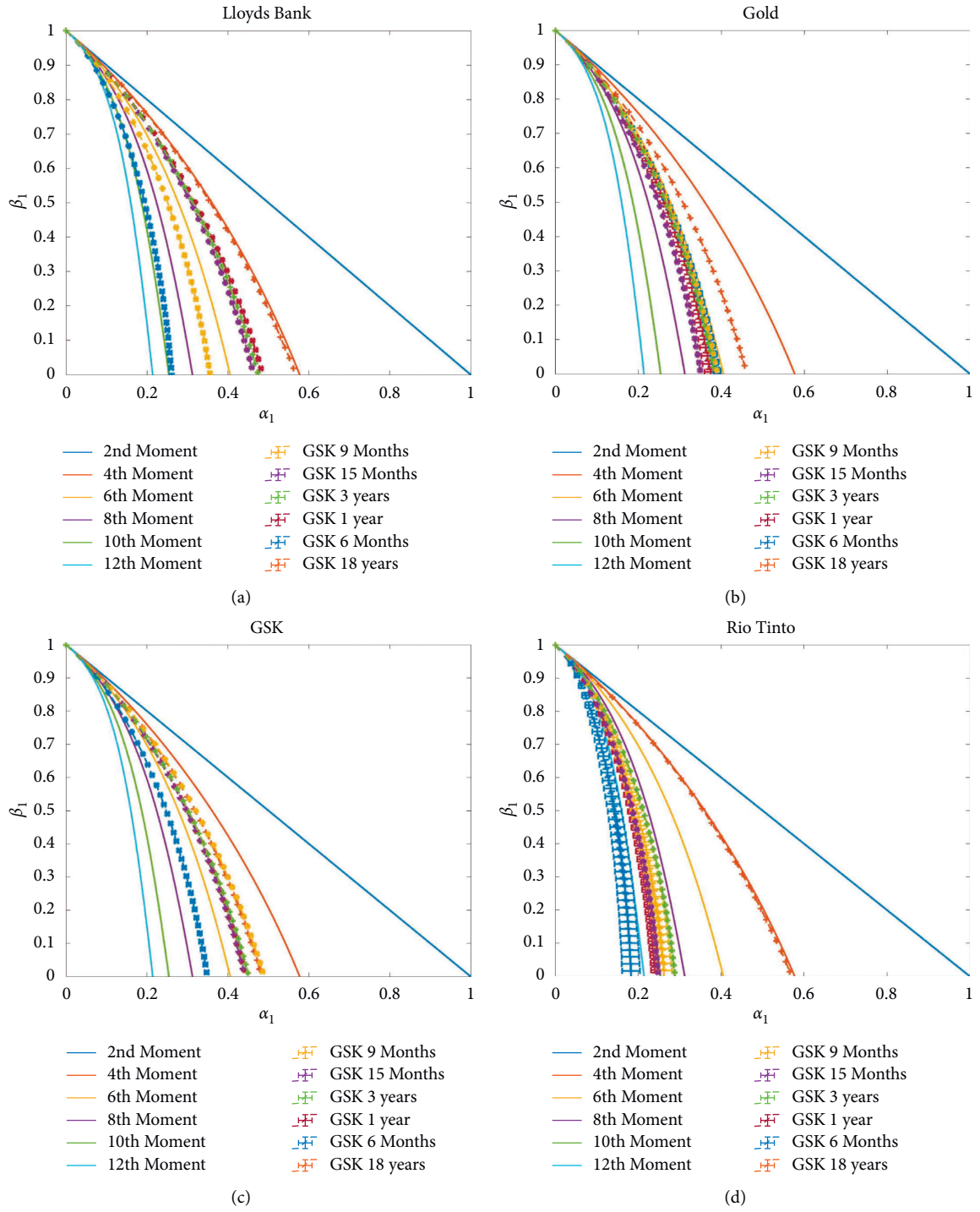

FIGURE 3: The stability phase diagram for the GARCH-normal (1,1) moments with an overlap of several company trajectories. (a) The trajectory for Lloyds Bank, where the shortest time window allows up to the tenth-order moment to exist. (b) The trajectory of Gold ETFs (Exchange Traded Funds), where the shortest time window allows to the sixth moment to exist. (c) The same for GSK, which allows up to the sixth moment to exist and lastly. (d) The same for Rio Tinto, which allows up to the twelfth-order moment to exist. We also show the error intervals of the trajectories, see Appendix A for details.

To find the value of α_0, this method is inspired by the trajectory analysis we use in the previous section. We search for α_0 by traversing the trajectory and trying to fit the empirical sixth-order standardised moment. However, if Γ_6 is lower than the minimum or larger than the maximum of possible Γ_6 stated in Table 1, this equation cannot be solved, indicating that the GARCH-normal model with such a value of the empirical sixth-order standardised moment does not exist.

In the second approach to fit empirical values of $\langle x^2 \rangle$, Γ_4 and Γ_6, we first fit the empirical fourth- and sixth-order

Table 1: The minimum and maximum values of Γ_6 along the company's trajectories in (α_1, β_1) space.

Company	Minimum	Maximum
Lloyds-6 months	33.3700	37.0000
GSK-6 months	60.3386	76.5162
Gold-3 year	90.3439	253.4463
Gold-1 year	79.3684	188.9430
RioTinto-3 year	36.1730	42.5383
RioTinto-1 year	34.1419	39.9972
RioTinto-6 months	30.9564	35.3291

standardised moments using the fact that $\Gamma_4(\alpha_1, \beta_1)$ and $\Gamma_6(\alpha_1, \beta_1)$ do not depend on α_0, see equations (9) and (10). Therefore, we can reduce the problem to two equations:

$$\begin{aligned} \Gamma_4(\alpha_1, \beta_1) &= \Gamma_{4,\text{emp}}, \\ \Gamma_6(\alpha_1, \beta_1) &= \Gamma_{6,\text{emp}}. \end{aligned} \tag{14}$$

Allowing us to evaluate values of α_1, β_1 and reserve α_0 to the fitting of variance: $\alpha_0 = \sigma^2_{\text{emp}}(1 - \alpha_1 - \beta_1)$. The set of equations (14) can be further reduced to one equation by eliminating β_1 using the first equation of the set namely

$$\beta_1 = \sqrt{1 - 2\alpha_1^2 - \frac{6\alpha_1^2}{\Gamma_{4,\text{emp}} - 3}} - \alpha_1, \tag{15}$$

And substitute it to the second equation of (14). This enables us to write the one-variable equation:

$$\Gamma_6\left(\beta_1\left(\alpha_1, \Gamma_{4,\text{emp}}\right), \alpha_1\right) = \Gamma_{6,\text{emp}}. \tag{16}$$

Note, we similarly can exclude α_1, resulting in equations for β_1.

4.3. Phase Diagram. Equations (14) can only be solved for some region, in standardised moment space, (Γ_4, Γ_6), which is the region between the black lines in Figure 4(a). This is the region of phase space where the respective values of the fourth- and sixth-order standardised moments can be fitted by a GARCH-normal model. For example, the first point $(1.7, 8)$ is inside the "GARCHable" region. However, the second point $(2.5, 8)$ is outside of the "GARCHable" region, highlighting that these moment values cannot be fitted by a GARCH-normal model. Therefore, no solution is possible to equations (14).

To evaluate the appropriateness of a GARCH-normal (1,1) model for the fitting of higher order moments in stock market data, we shall be investigating time series for companies of different sectors of the economy by estimating their empirical values of the fourth- and sixth-order standardised moments and comparing with the GARCH-normal (1,1) parameter region in (Γ_4, Γ_6) space, Figure 4(a). To see the effect of the length of the time window on the ability of the GARCH-normal (1,1) model to fit empirical moments, we study data in different economic periods. We start by taking a time window of 1% of the overall time series and increment in percents up to its full length (see Figure 5), an example of this can be seen for the several stocks in Figure 4(a), [30], ignoring time windows shorter than 30 days. We then overlap these data points on top of the "GARCHable" region detailed above. It can be seen from Figure 4(b), the distribution of empirical data points highlights a distinct corridor where the data sits. We generate much more information by this method than working out the errors using a standard error procedure. In fact, we see distinct areas in the parameter space where more empirical data points reside than others. We further show by this method there are only very specific regions where the empirical data lies, and it does not span all of the parameter space, seen by the grid of points in Figure 4(b).

We do not see the empirical data inside of the GARCH-normal (1,1) phase region for the time period analysed. Therefore, we can say that a GARCH-normal (1,1) model is unable to simultaneously fit three even higher order moments of the empirical time series we have studied.

5. GARCH-Double-Normal Models

Since we cannot fit the fourth- and sixth-order standardised moments with the GARCH-normal (1,1) model, we consider a GARCH model with the more flexible double Gaussian conditional distribution. Such GARCH-double-normal models have been extensively researched [31–33], where the authors use them for volatility and exchange rate modelling. The conditional double Gaussian distribution can be written as

$$p(x) = \frac{a}{\sigma_1\sqrt{2\pi}} e^{\left(-x^2/2\sigma_1^2\right)} + \frac{b}{\sigma_2\sqrt{2\pi}} e^{\left(-x^2/2\sigma_2^2\right)}. \tag{17}$$

In addition to an obvious normalisation condition:

$$a + b = 1, \tag{18}$$

we also have constraints on the second moment:

$$E\left[x^2\right] = a\sigma_1^2 + b\sigma_2^2 = 1. \tag{19}$$

Due to the requirement that the conditional distribution for a GARCH process should have variance equal to one. We can introduce two more convenient parameters (the 4th and 6th moments of the conditional distribution) which fully define the distribution in (17):

$$E\left[x^4\right] = a\sigma_1^4 + b\sigma_2^4 = \mu_4 = \frac{\eta_4}{3}, \tag{20}$$

$$E\left[x^6\right] = a\sigma_1^6 + b\sigma_2^6 = \mu_6 = \frac{\eta_6}{15}. \tag{21}$$

The parameterisation (20) and (21) of the double Gaussian distribution allows us to generalise Bollerslev's equation (9). The second-order moment σ^2 is not affected and is still determined by equation (8), while the fourth- and sixth-order standardised moments for GARCH with double-Gaussian distribution can be written as

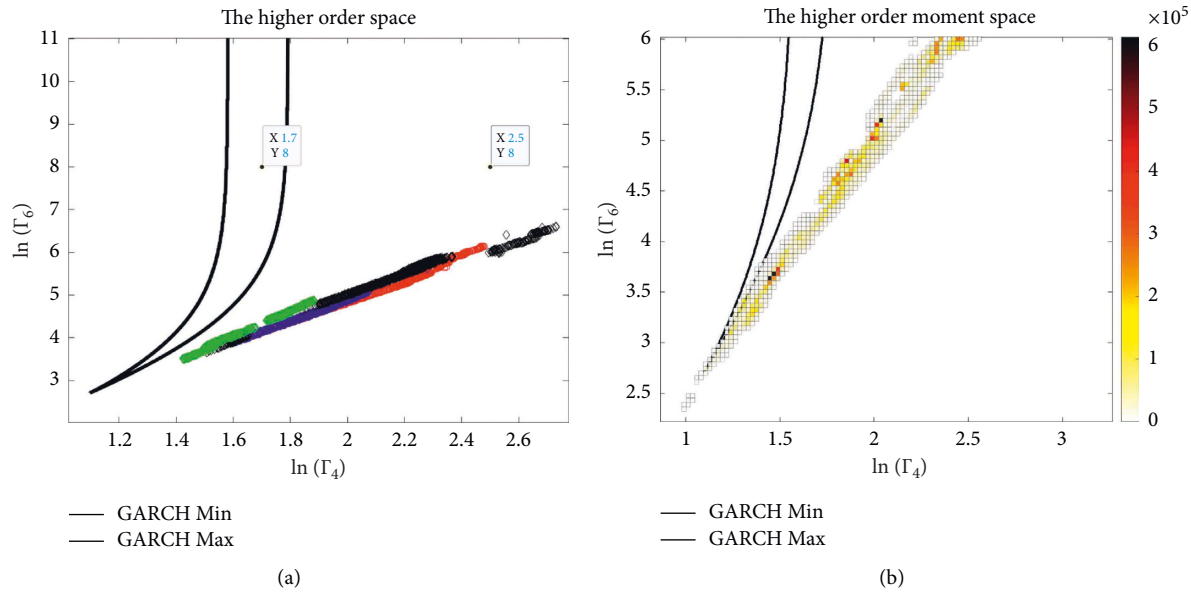

Figure 4: In (a), the phase diagram for $(\ln(\Gamma_4), \ln(\Gamma_6))$ space. The enclosed area between the black lines shows the region in which the GARCH-normal model is able to fit the fourth- and sixth-order standardised moment, whilst the rest of the space is where the values of Γ_4 and Γ_6 cannot be fitted by a GARCH-normal (1,1) model. The two highlighted points $(1.7, 8)$ and $(2.5, 8)$ show the examples of values of Γ_4 and Γ_6 that can be fitted by a GARCH-normal model and those that cannot, respectively. The other data points in the space represent the empirical data for several companies, truncated to 1% of its overall length, incrementing in percents up to its full length. In (b), we show the histogram for point density on the higher order moment phase space, we detail the specifics of this calculation in A. We consider all possible windows with duration longer than 30 days. We show the histogram alongside the "GARCHable" region. The empirical data is shown for Lloyds Bank, GSK, Barclays Bank, Gold ETFs, S&P 500, DowJones, Rio Tinto, Bank of America, Oil, Natural Gas, Vale, Pfizer, and Citi Bank. This histogram shows the scattering of empirical data in a much clearer way than any error bar estimation, in which some information about the point distribution is lost.

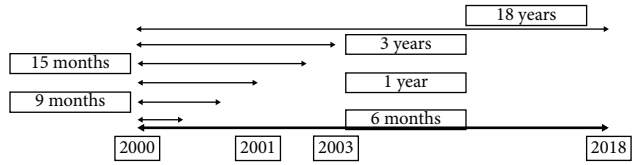

Figure 5: The timeline of time-series windows that we investigate within the study. We investigate the periods of economic turmoil as well as relatively stable periods. We also highlight here the truncation of 18 years, 3 years, 15 months, 1 year, 9 months, and 6 months.

$$\Gamma_4 = \frac{\eta_4 (1-\alpha_1-\beta_1)^2 (1+(2(\alpha_1+\beta_1)/1-\alpha_1-\beta_1))}{1-\eta_4\alpha_1^2-2\alpha_1\beta_1-\beta_1^2}, \tag{22}$$

$$\Gamma_6 = \frac{\eta_6 (1-\alpha_1-\beta_1)^3 \left(1+(3(\alpha_1+\beta_1)/1-\alpha_1-\beta_1)+3\left(1+\left(2(\alpha_1+\beta_1)\left(\eta_4\alpha_1^2+2\alpha_1\beta_1+\beta_1^2\right)/1-\eta_4\alpha_1-2\alpha_1\beta_1-\beta_1^2\right)\right)\right)}{1-\eta_6\alpha_1^3-3\eta_4\alpha_1^2\beta_1-3\alpha_1\beta_1^2-\beta_1^3}. \tag{23}$$

Using the methods described prior and based on the existence of solutions of the set of equations (14) with the corresponding standardised moments, defined by equations (22) and (23), we create a family of phase diagrams parameterised by η_4 and η_6. To understand which empirical values are achievable using a GARCH-double-normal model, we need to understand restrictions for the whole family of phase diagrams. We see that these are bounded due to limitations for η_4 and η_6 obtained in Appendix D (conditions 43 and 44). These limitations require all phase diagrams be started from points above the dashed line, Figure 6. As such only data above the dashed line can be described by a GARCH-double-normal model (which is the case for the empirical data collected for the securities we have considered here).

5.1. Time Windows. In Figure 6, we see three-parameter diagrams for three different double Gaussian distributions. Parameters for these diagrams are given in Table 2.

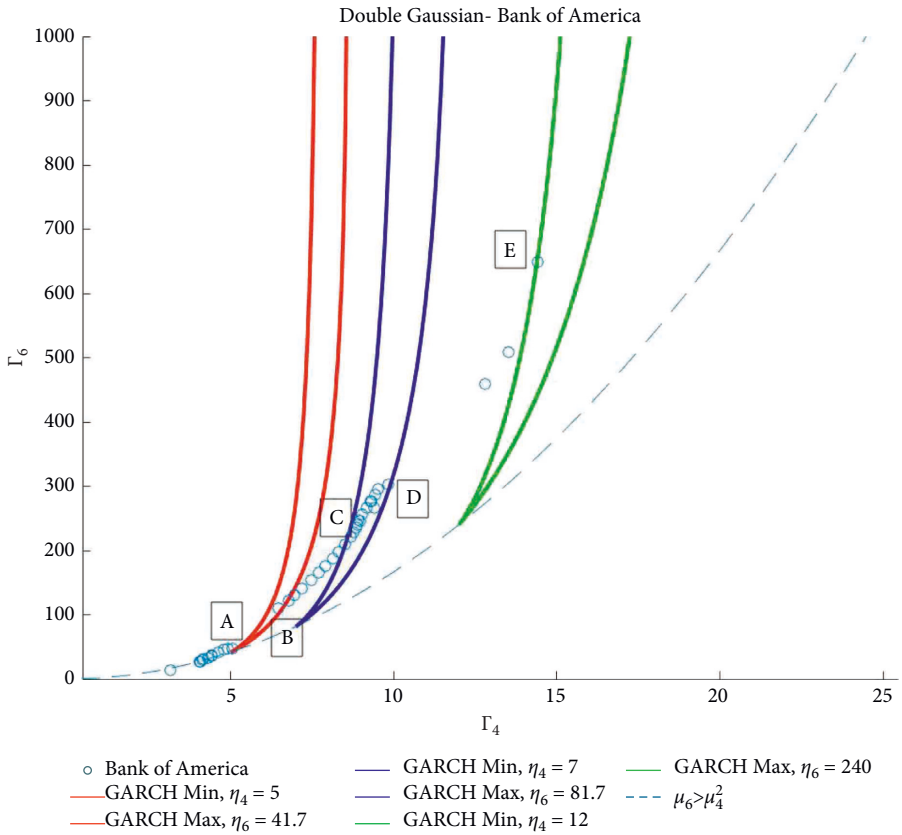

FIGURE 6: The phase diagrams for (Γ_4, Γ_6) space for GARCH-double-normal (1,1) models corresponding to different parameters given in Table 2. We overlay the empirical data for Bank of America, truncated from 1% to 100% of the length of the time series, incremented in one percent steps, for the period of 6 October 2000 to 6 October 2018. To highlight the ability of the GARCH-double-normal model to fit higher order moments for specific lengths of time windows, we present three regions for the space that allow the fitting of the fourth- and sixth-order standardised moments by a GARCH-double-normal model. Each has a different time window that it can fit, shown by the letter, associated with Table 2.

TABLE 2: Parameters of the conditional double Gaussian distributions used to construct "GARCHable" regions in Figure 6.

Position	η_4	η_6	$t_{\min}$ (days)	$t_{\min}$ (days)
Leftmost (red)	5	41.7	171 (A)	600 (B)
Centre (blue)	7	81.7	943 (C)	1500 (D)
Rightmost (green)	12	240	1586 (E)	

The table summarises the parameters of the distributions used to model the time windows (A) to (B), (C) to (D), and from (E). These are the limits of the time windows in days that the particular instance of the double Gaussian distribution can be used to fit the higher order moments of the empirical data of the Bank of America.

Figure 6 demonstrates how altering the parameters η_4 and η_6 of the GARCH-double-normal model enables us to capture different time windows of the empirical data. The data used in Figure 6 is for the Bank of America time series from 6 October 2000 to 6 October 2018. We truncate the time series into different lengths. We start with 1% of the overall length and increment by 1% up to the whole length of the time series. In other words, the first, most left point, corresponds to 43 days of data (from 06/10/2000 to 04/12/2000), the second point corresponds to moments obtained for 86 days of data (from 06/10/2000 to 31/01/2001), and so on. For the leftmost phase diagram, we use a double Gaussian distribution with $\eta_4 = 5, \eta_6 = 41.7$. This allows us to fit σ^2, Γ_4 and Γ_6 for the time window of duration in the interval, $171 \leq t \leq 600$ days. When fitting higher order moments for longer time windows, we need to use double Gaussian distributions with parameters summarised in Table 2. It is not possible to gain a GARCH process with a double Gaussian distribution to capture all of the empirical data's higher order standardised moments. We denote this behaviour as the local ability to model higher order moments of financial time series by the GARCH-double-normal model. Figure 6 only uses the data from the Bank of America; however, this behaviour is seen throughout the empirical data we have studied. In order to capture the empirical data, we must first decide on the time window we wish to model and then ascertain a suitable distribution that will capture this window.

5.2. Time Dependence of GARCH-Double-Normal Parameters. Once we have fixed the time window we wish to analyse, we can study what happens when the window with this fixed duration shifts in time. This can be done by attributing to the higher order moments a time moment, t, corresponding to the middle point (the median) of the time window, see equation (1). This can be seen in Figure 7, where we detail the schematic of a fixed time window moving in time for a long time series.

If we fix the double Gaussian distribution (in essence, select certain η_4 and η_6), we can gain the set of GARCH parameters, α_0, α_1 and β_1 that describes the particular time median. If we change the time window we look at by moving its time median, then the GARCH parameters α_0, α_1, and β_1 also change. Below, we observe that the GARCH parameters $\alpha_0(t)$, $\alpha_1(t)$, and $\beta_1(t)$ significantly vary with the moving time window, highlighting the nonstationarity of our modelling.

Given equations (8) and (22), we are able to define trajectories in (α_1, β_1) space for a fixed value of σ^2_{emp} and $\Gamma_{4,\text{emp}}$. Unlike the GARCH-normal methods, we now have the trajectories which change when η_4 varies. These can be seen below:

$$\alpha_1 = \sqrt{\frac{\left(\left(2\alpha_0/\sigma^2_{\text{emp}}\right) - \left(\alpha_0/\sigma^2_{emp}\right)^2\right)\left(\Gamma_{4,emp} - \eta_4\right)}{\left(\Gamma_{4,\text{emp}} - \eta_4\right)\left(\eta_4 - 1\right) - \left(\eta_4^2 - \eta_4\right)}}, \tag{24}$$

$$\beta_1 = 1 - \frac{\alpha_0}{\sigma^2_{\text{emp}}} = \sqrt{\frac{\left(\left(2\alpha_0/\sigma^2_{\text{emp}}\right) - \left(\alpha_0/\sigma^2_{emp}\right)^2\right)\left(\Gamma_{4,emp} - \eta_4\right)}{\left(\Gamma_{4,\text{emp}} - \eta_4\right)\left(\eta_4 - 1\right) - \left(\eta_4^2 - \eta_4\right)}}. \tag{25}$$

Now for each desired dataset we can use the trajectories in the same manner as we have done with the GARCH-normal model. We can plot Γ_6 along the trajectories of (α_1, β_1) using the running parameter α_0, overlaying this with the empirical value (see Figure 8).

From the above method, we can recover the value of $\alpha_0(t)$ that allows the fitting of $\sigma^2_{\text{emp}}(t)$, $\Gamma_{4,\text{emp}}(t)$, and $\Gamma_{6,\text{emp}}(t)$, where t is the median of the running window, enabling us to create Figure 9. This is done for several banks: Lloyds Bank, Barclays Bank, and Bank of America, and a commodity, Gold ETFs. We seek to find a fingerprint of the companies' GARCH parameters through the financial crisis. It is evident from Figure 9 that the banking sector has a unique behaviour in response to the crisis. We see an initial flat signal, but when the crisis period occurs we see an increase in the parameter value followed by a very dramatic reduction. This behaviour is mirrored in the commodity, Gold. We propose to use this specific behaviour exhibited by the banking companies as an indicator for future banking crisis periods. In Figure 9, we highlight an interval of the α_0 value which reflects the error interval of the α_0 parameter. This was recovered using the same method as described in Appendix A, the interval reflects the maximum and minimum values, a similar method to that used in Figure 1.

6. Likelihood Estimations for Γ_4 and Γ_6

Here, we consider a likelihood estimation for the parameters of a GARCH model using higher order moments. We focus on the procedure of fitting when the empirical data is located outside of the "GARCHable" region of the GARCH-normal (1,1) process shown in Figure 5(b). As we can see from below, the Maximum Likelihood Estimators (MLE) and the methods outlined in this study are the same when we are inside the "GARCHable" region. However, when the empirical points are outside of this region, each of the methods presented above does not allow us to estimate the GARCH parameters. In this section, we will analyse if and how a likelihood estimate can resolve the issue.

If we follow the method of error estimation described in appendix A, we need to shift a central point of the studied time window. For each central point of the studied time window we estimate the $\Gamma_{4,\text{emp}}$, $\Gamma_{6,\text{emp}}$. Considering an ensemble of these moments for different central points as a dataset, we estimate the mean values, $\Gamma^{\mu}_{4,\text{emp}}$, $\Gamma^{\mu}_{6,\text{emp}}$, the standard deviations $\sigma_{4,\text{emp}}$, $\sigma_{6,\text{emp}}$ and the mutual Pearson correlation coefficient ρ, of these time windows. The statistics of the studied data points of the fourth and sixth have not been investigated as of yet. In the absence of such a study, we assume that the data's distribution can be approximated by a bi-variant Gaussian function. To fit this distribution to the data, we can maximise the corresponding cost function, which is in line with the common use of the Maximum Likelihood Estimation (MLE). As such, we can follow the MLE methods, [21, 23], and derive a cost function that needs to be optimised:

$$\mathscr{F} = \frac{\left(\Gamma_4 - \Gamma^{\mu}_{4,\text{emp}}\right)^2}{\sigma^2_{4,\text{emp}}} - 2\rho\frac{\left(\Gamma_4 - \Gamma^{\mu}_{4,\text{emp}}\right)\left(\Gamma_6 - \Gamma^{\mu}_{6,\text{emp}}\right)}{\sigma_{4,\text{emp}}\sigma_{6,\text{emp}}} + \frac{\left(\Gamma_6 - \Gamma^{\mu}_{6,\text{emp}}\right)^2}{\sigma^2_{6,\text{emp}}}. \tag{26}$$

Moreover, if we take the derivative of this cost function with respect to α_1 and β_1 and setting the derivatives equal to zero, we will recover equations (14) (section 4.2), which have solutions inside of the "GARCHable" region. Note, if we assume that the fourth- and sixth-order standardised moments are distributed according to a Gaussian law, the minimum of the cost function (26) will correspond to the maximum probability density. Furthermore, based on the cost function we can define a distance as:

$$\mathscr{L}^2 = \left(X - X_0\right)^2 - 2\rho\left(\left(X - X_0\right)\left(Y - Y_0\right)\right) + \left(Y - Y_0\right)^2. \tag{27}$$

By defining, $X = \Gamma_4/\sigma_{4,\text{emp}}$, $X_0 = \Gamma^{\mu}_{4,\text{emp}}/\sigma_{4,\text{emp}}$, $Y = \Gamma_6/\sigma_{6,\text{emp}}$ and $Y_0 = \Gamma^{\mu}_{6,\text{emp}}/\sigma_{6,\text{emp}}$. Since we consider a GARCH process, we have to assume, $\Gamma_4 = \Gamma_4(\alpha_1, \beta_1)$ and $\Gamma_6 = \Gamma_6(\alpha_1, \beta_1)$ described by equations (9) and (10), respectively. We have used a similar algorithm to that defined in the phase diagram section to find the minimum distances between the "GARCHable" region and the empirical data.

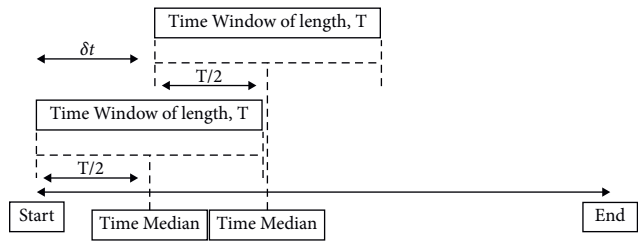

FIGURE 7: Here, we show how we take a rolling window for a long time series (from the start to the end). We highlight two fixed time windows, of certain length, T, with time median that corresponds to the middle of these windows. This time window then shifts in time, by δt, taken here to be six months.

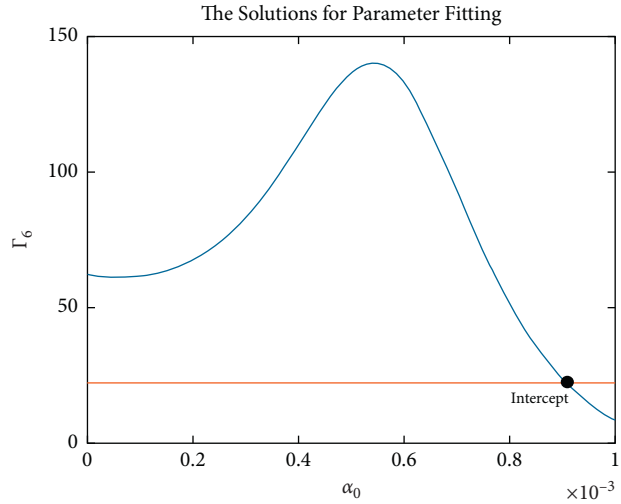

FIGURE 8: Γ_6 as a function of the running parameter α_0. Here, we show how we calculate the value of α_0 for a particular time window. The orange line is the value of Γ_6 for the empirical time window, $\Gamma_6 = \Gamma_{6,\text{emp}}$, whilst the blue line shows $\Gamma_6(\alpha_0)$, equation (23) when $\alpha_1 = \alpha_1(\eta_4, \alpha_0, \sigma^2_{\text{emp}}, \Gamma_{4,\text{emp}})$ (equation (24)) and $\beta_1 = \beta_1(\eta_4, \alpha_0, \sigma^2_{\text{emp}}, \Gamma_{4,\text{emp}})$ (equation (25)), for the GARCH-double-normal model. The intercept of the two lines shows the value of α_0 which allows us to model data for a certain median time and a certain time window within the GARCH-double-normal (1,1) model.

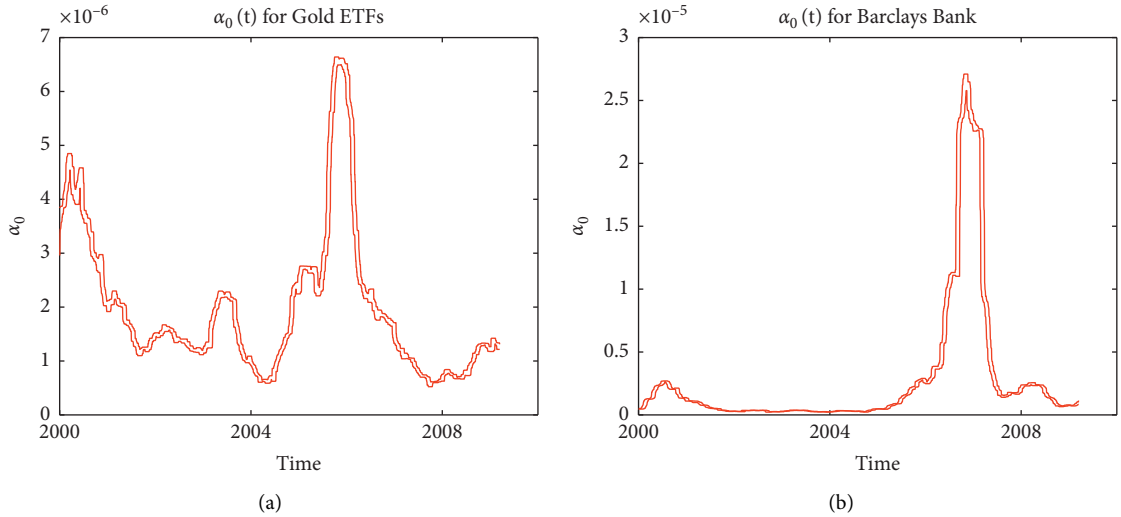

FIGURE 9: The evolution of the GARCH parameter α_0 for the period 2000–2009. The two plotted curves provide the upper and lower bounds of the confidence interval for α_0 estimated by the method described within Appendix A, for Gold ETFs (a) and Barclays Bank (b). In all figures, we see a large increase in the value of α_0 prior to the financial crisis of 2008, followed by a very large decrease either before or during the crisis period.

The values α_1 and β_1, which minimise the distance L, could be considered as the best likelihood estimation of the parameters. We have investigated the dependence of the minimum distance $\mathscr{L}_{\min}$ on the size of empirical data collection windows for Gold ETFs and Barclays Bank (see Figure 10). The distances exceed 1 indicating the low probability of the system described by the GARCH process in agreement with our conclusions above.

When we study the empirical data we discover the empirical values of the fourth- and sixth-order standardised moments are highly correlated, $\rho \approx 1$, see insert of Figure 10. This is to be expected since both higher order standardised moments are affected by rare-events within our time series. As such, if the number of rare-events increases so does the value of both higher order standardised moments. Due to this high level of dependence (correlation) between our random variables ($\Gamma^{\mu}_{4,\text{emp}}$ and $\Gamma^{\mu}_{6,\text{emp}}$), we can evaluate the probability of fitting our GARCH model to empirical data using higher order standardised moments by just one of the random variables. If we choose to use Γ_4 as our random variable and assuming this variable is to follow the distribution: $p(X) = (1/\sqrt{2\pi\sigma_{4,\text{emp}}})e^{-(X-X_0)^2}$, where X and X_0 are defined as above. When we calculate such values, we see the values of the probability being low $(p(x) \sim 10^{-3})$, highlighting our conclusion that fitting empirical data by a GARCH-normal (1,1) model is very unlikely when we wish to fit higher order standardised moments.

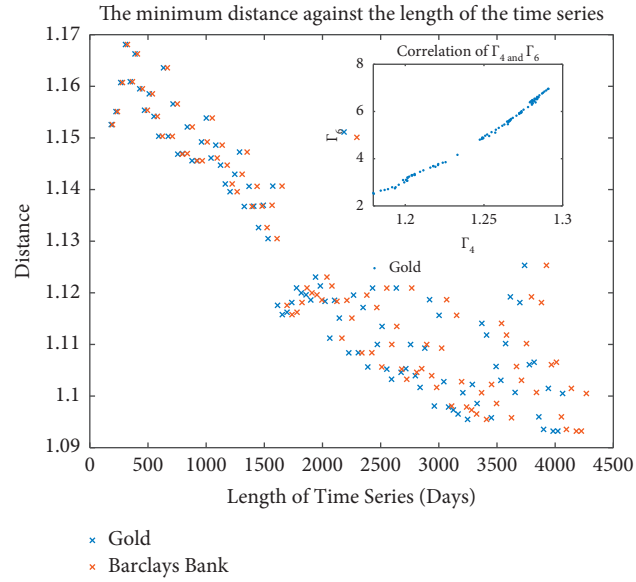

Figure 10: The minimum distance of two time series, Barclays Bank (red) and Gold ETFs (blue) between 2000 and 2018, when we truncate the time series into different lengths, is shown for the cost function (27). An insert of this plot highlights the correlation between Γ_4 and Γ_6 for Gold ETFs, which corresponds to a correlation coefficient, $\rho = 0.9953$.

7. Analysis of COVID-19 Time Window

The study focusses primarily upon the 2008 financial crash; however, in recent times, the world has undergone a much more profound economic and social shock, the COVID-19 pandemic. It is reasonable to assume, the pandemic would create a similar, if not greater, impact on economic and financial systems, given the nature of the crisis period. Therefore, we carry out the analysis, namely, deriving the time evolution of the GARCH parameter, α_0 and the time evolution of the sixth-order standardised moment for the empirical time series of several stock instruments within the COVID-19 pandemic time period.

In Figure 11, we show the sixth-order standardised moments for Lloyds Bank, Barclays Bank and the Bank of America for the period 2019–2021. In each panel, we show the error interval using the same method described previously. It can be seen that Barclays Bank and the Bank of America show quintessential features of their sixth-order standardised moment evolution that is indicative of a crisis period: a sharp increase, followed by a sharp decrease around the start of the pandemic. Whereas, Lloyds Bank sees a steadier increase followed by a sharp decrease further into 2020, this could be attributed to the U.K.'s handling of the pandemic, as the UK did not go into lockdown until March 2020.

We also investigate the evolution of the GARCH parameter, α_0 in the same time period. In Figure 12, we see the evolution of α_0 for Lloyds Bank, Barclays Bank and the Bank of America. It can be seen that in all empirical time series analysed, we recover the signal of the crisis period: a sharp increase followed by a sharp decrease, around the start of the pandemic. A strong indication of a crisis period affects the instruments.

In Figure 13, we show the time evolution for the sixth-order standardised moment and the GARCH parameter α_0 for the S & P 500 for the COVID-19 pandemic and the financial crash of 2007–2009. In panel (a), we can see that when the pandemic started, around 2020, we gain a large increase in the moment's value. This is followed by a very sharp decrease in the value. Whilst in panel (b), we show the evolution of the GARCH parameter α_0, we see a very similar behaviour compared to the banking stocks of the same period. A sharp increase is seen in the parameter value, followed by the now expected sharp drop around the start of the crisis period.

In panel (c), we detail the behaviour of the sixth-order standardised moment for the index over the period 2004–2012. It can be seen that the sixth-order standardised moment is very noisy and as such, we are unable to determine any behaviour that could allude to the type of economic environment the index inhabits at this instance in time. This can be attributed to the structure of the index. The S&P 500 index is the 500 largest companies by market capitalisation, within the United States of America as ranked by Standard and Poor's credit agency. Therefore, a plethora of different sectors will be represented in such an instrument. This means that sectors which would normally be at risk from financial crises, for example banks, will be mitigated by the other sectors within the index. Moreover, in panel (d), we show the evolution of the GARCH parameter, α_0 in time. For this parameter's evolution, we see a similar

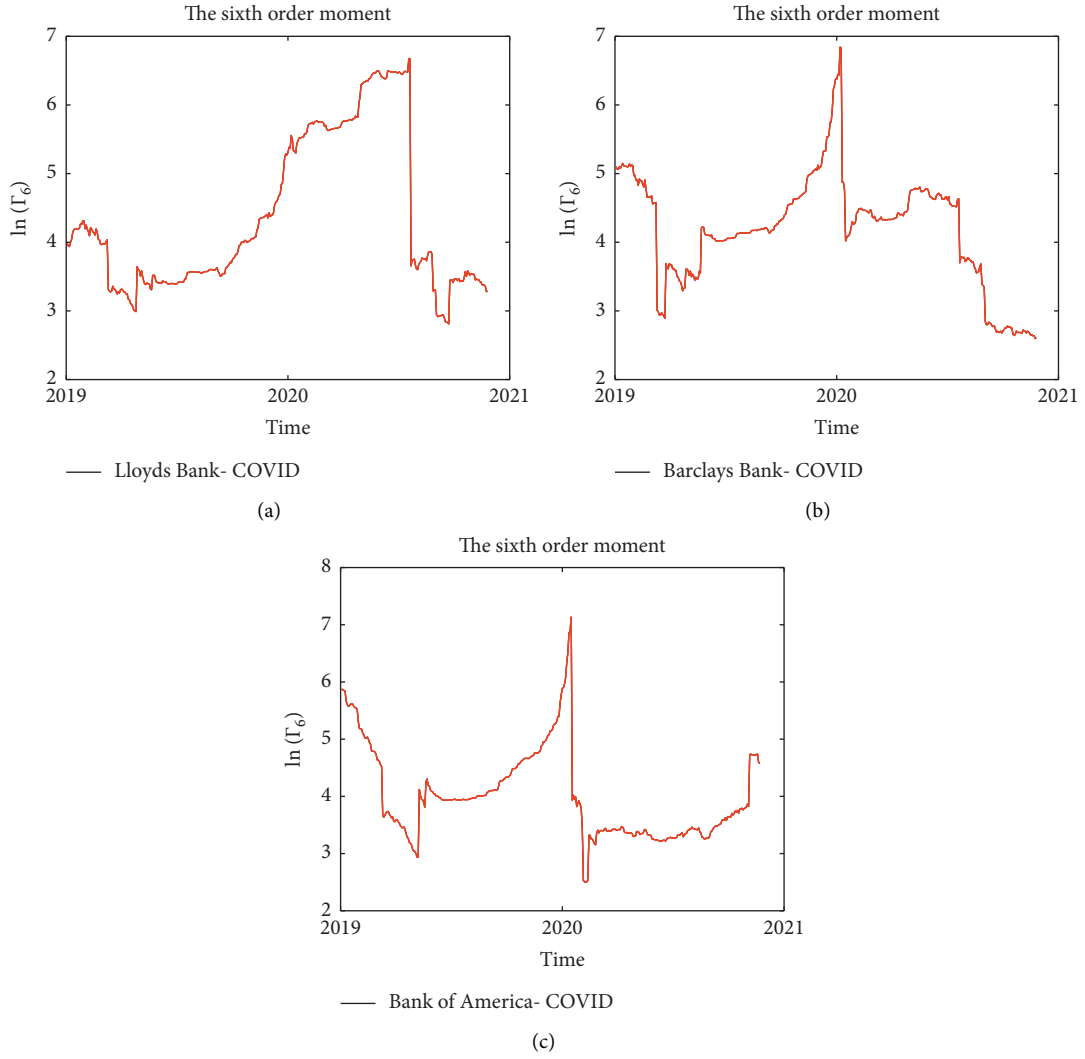

FIGURE 11: The time evolution for the sixth-order standardised moments for the period 2019–2021, the COVID-19 pandemic. In panel (a), we show the analysis for Lloyds Bank, (b) details the same for Barclays Bank, and finally (c) shows the Bank of America. In panels (b) and (c), we see the sharp increase followed by a decrease, which is the representative of an economic crisis being present, this is around the start of the pandemic. However, Lloyds Bank does not necessarily follow this and instead, we see a steady increase followed by a sharp decrease further into 2020. This could be attributed to the U.K.'s slow handling of the pandemic.

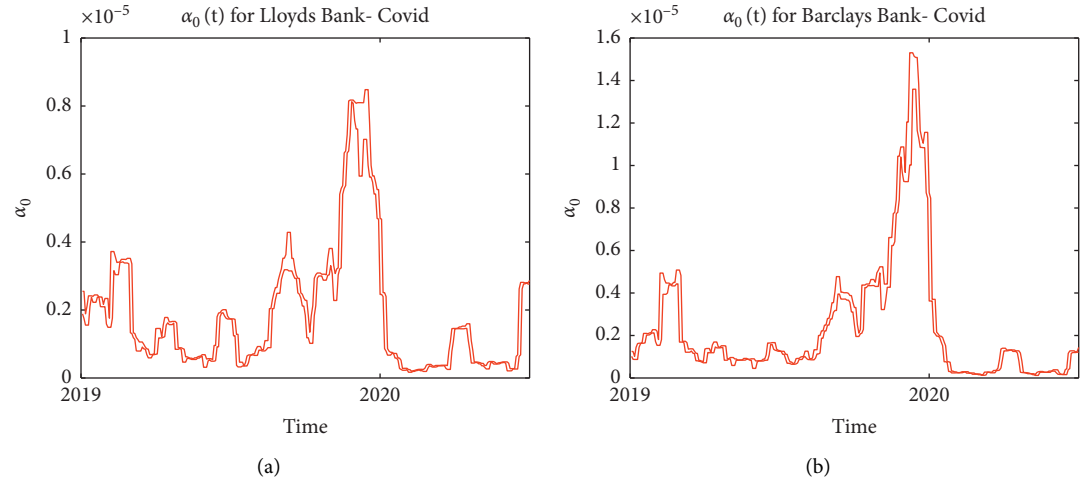

FIGURE 12: Continued.

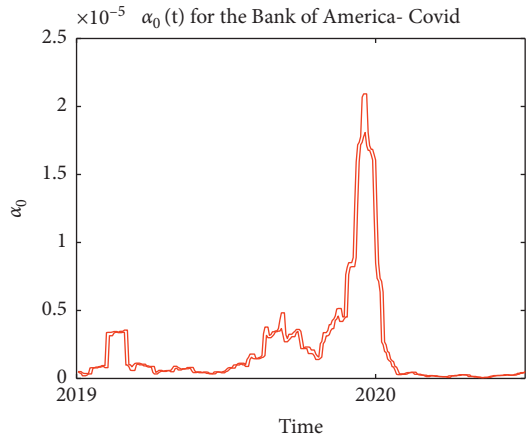

(c)

Figure 12: The GARCH parameter's (α_0) time evolution for Lloyds Bank (a), Barclays Bank (b), and the Bank of America (c) for the period 2019–2021. In all panels, we see the typical α_0 signal for a crisis period. There is a very high peak of the parameter value around the start of the crisis period. In all time series analysed, we detail the error interval for the parameter's value, using the method described previously.

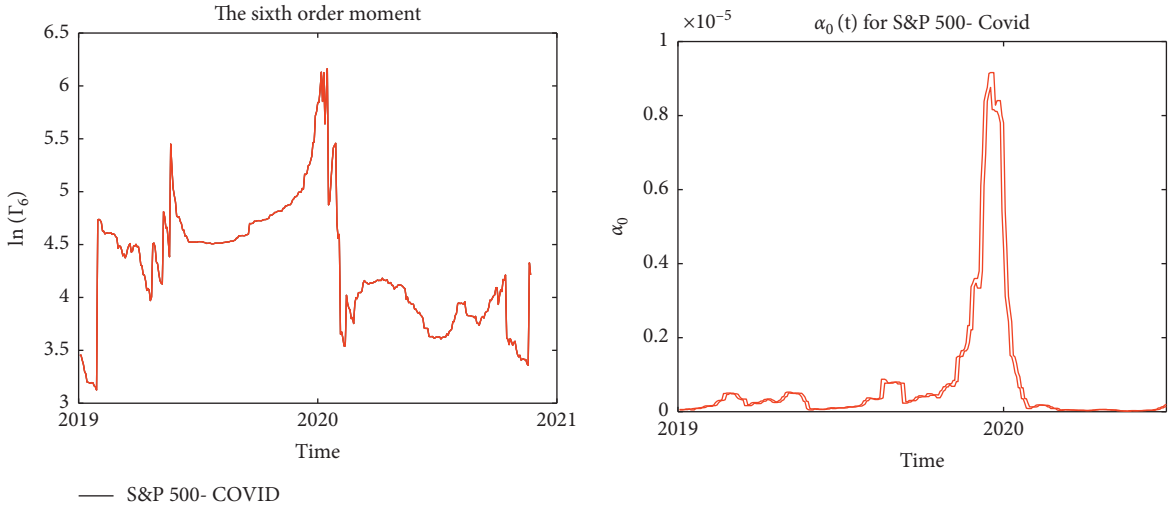

(a) (b)

Figure 13: Continued.

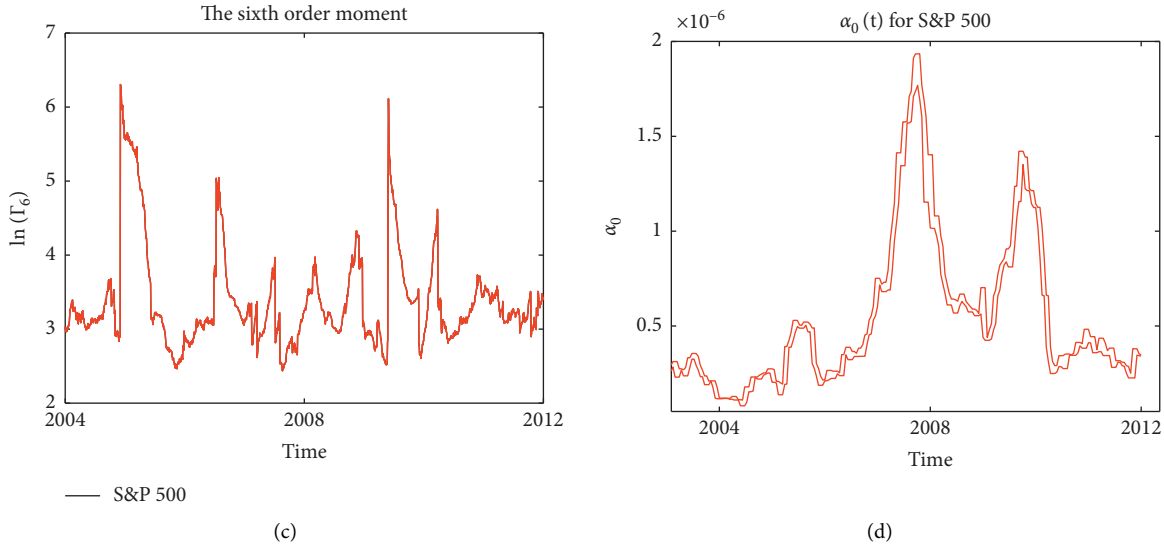

FIGURE 13: The evolution of the sixth-order standardised moment and GARCH parameter α_0 throughout the COVID-19 pandemic. (a) The sixth-order standardised moment evolution for the COVID-19 pandemic period. (b) The evolution for the GARCH parameter for the same period. The behaviour seen is in agreement with the banking stocks through the financial crisis of 2008. (c) The behaviour of the sixth-order standardised moment for the S&P 500 stock index through the 2008 financial crisis. We see a very noisy signal for much of the time period analysed. (d) The evolution of the GARCH parameter, α_0. We show the analysis for the parameter for the period 2004 to 2012. The parameter evolution for the S&P 500 shows a similar dynamic to the pandemic period. However, the peak is an order of magnitude lower than seen in the COVID-19 pandemic period.

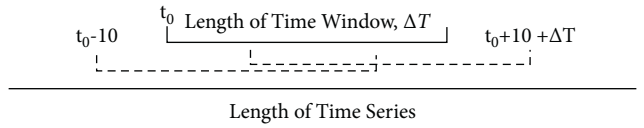

FIGURE 14: The schematic for the calculation of the error bars for the time window of length, ΔT, with a starting position, t_0. We displace the window by $\pm i$, where $i = 0 - 10$ days, and work out the value of the moments for this window. We take either the raw values of the moments and the maximum and minimum values of the range or the standard deviation of this, as described in the text.

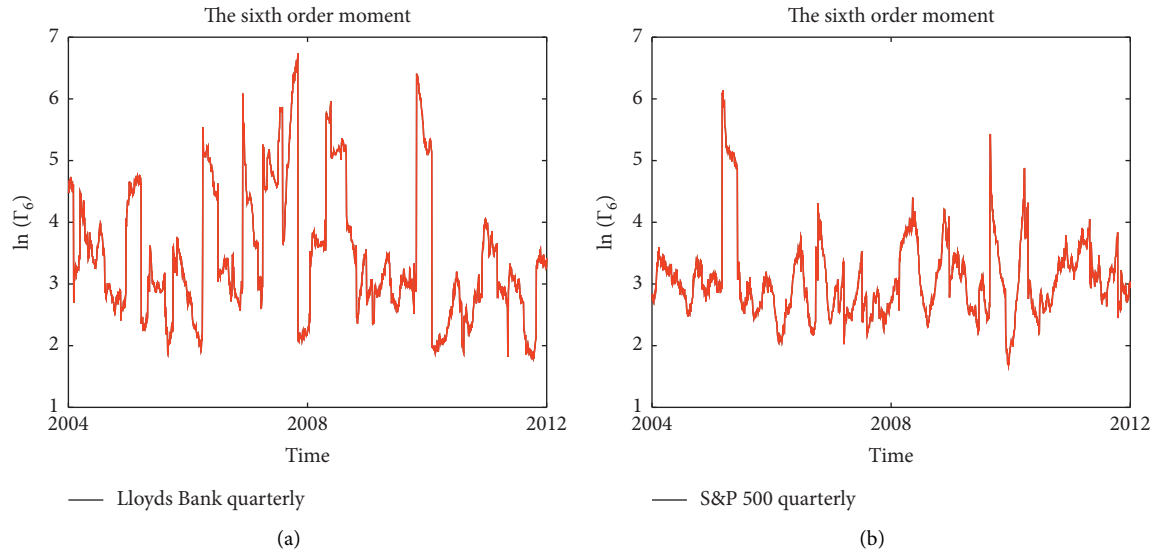

FIGURE 15: The time evolution of the sixth-order standardised moment for Lloyds Bank, panel (a) and the S&P 500 index, panel (b), when we truncate the long 18-year time series into quarterly time windows (around 63 days).

response as has been seen within the COVID-19 pandemic, an increase in the value of the parameter followed by a decrease. However, the magnitude of increase and decrease is much smaller than for the COVID-19 period.

In the two crisis periods studied, we gain different responses for the index's sixth-order standardised moment, but gain a similar behaviour in its GARCH parameter evolution α_0, albeit some difference in the scaling of the parameter. In the COVID-19 pandemic, all sectors of the economy were affected and as such, the index's sixth-order standardised moment reflects this. Whilst, the financial crisis of 2008 predominantly affected banking companies, so we see a reduced effect in the standardised moment. In addition, we can see that the COVID-19 peak is an order of magnitude higher than the peak gained in the banking crisis. Due to this observation, we can conclude that the GARCH parameter behaviour allows us to analyse the depth of the crisis, the larger the peak, the deeper the crisis penetrates into the economy for the analysis undertaken on this index.

8. Conclusion

We use the time series of The Bank of America, Barclays Bank, Citi Bank, HSBC, Gold ETFs, GlaxoSmithKlein and Lloyds Bank, among others, to highlight the inability of a GARCH (1,1) model with the Gaussian conditional distribution to fit higher order moments of empirical time series.

In discovering this, we turn our attention towards different conditional distributions to try to capture the empirical data's higher order moments. We show that with the use of a GARCH-double-normal model we can fit the empirical data's higher order moments. However, through this enquiry, we still cannot capture the long run dynamics of the empirical data. We show that it is only possible to fit a model to empirical data within certain time horizons. To model a different time horizon we have to change the parameters of the double Gaussian distribution we use.

Fixing the distribution within certain time horizons to enable the fitting of higher order moments, highlights that the obtained GARCH-double-normal (1,1) model describes a nonstationary process. Therefore, if we wish to describe a long time series by a GARCH-double-normal model, we have to truncate it to smaller time windows. In doing so, we have to potentially fit GARCH-double-normal models with different parameters (α_0, α_1 and β_1) to each time window. Therefore, we produce a time dependence of the GARCH model's parameters, for example, α_0. As such, we are able to build up a time signature of the α_0 parameter through the 2008 financial crash for several companies. We focus our attention on the banking sector to distinguish any shared behaviour in the evolution of α_0, through this crisis period. The banking companies' values of α_0 have a distinct behaviour from other sectors of the economy, giving hope of a standardised signal of these periods. It is seen through the banking sector's empirical data that before the financial crash there is an increase in α_0 and during the financial period, the value of α_0 reduces extremely quickly. A behaviour that is found among banking companies but not other securities' time series. Analysis undertaken upon the COVID-19 pandemic period reinforces this belief. This finding is potentially useful for either forecasting or predicting financial turbulence in economic periods.

Appendix

A. Error Bar Calculations

To calculate the error intervals for the plots in this study, we carried out a time kernel type calculation. For the time window we investigate, we displace the starting point, t_0 by a value between $[-10, 10]$. Therefore, we move the starting point by $t_0 \pm i$ where, $i = 0 - 10$ days. We are able to work out the value of the moments for each displaced time window. For the range of values of the moment we gain, we can either take all of the values of the moments and plot them, as seen in Figure 5(a), creating error "clouds" or we can calculate the maximum and minimum values and get an error interval, as seen in Figure 1. The schematic for this method can be seen in Figure 14.

We also detail within the study a method of using two dimensional histograms to show the point density of the empirical data in the (Γ_4, Γ_6) space versus the "GARCHable" region, see Figure 5(a). To do this, we displace the time window as described above and plot all of the moment values we gain from the displaced windows. Taking these and plotting a histogram of the empirical points we are able to show the number of points with certain moment values. To gain more points we move the time window more than the ten days highlighted above. In some cases we displace the window by 100 days.

B. Divergence Line Expressions

For the fourth- and sixth-order moment we can obtain the divergence line explicitly, and so derive:

$$\beta_1^{(4)} = \sqrt{1 - 2\alpha_1^2} - \alpha_1,$$

$$\beta_1^{(6)} = \frac{\left(-8\alpha_1^3 + \sqrt{96\alpha_1^6 - 16\alpha_1^3 + 1} + 1\right)^{1/3}}{2^{1/3}} - \alpha_1 - \frac{2\,(2)^{1/3}\alpha_1^2}{\left(-8\alpha_1^3 + \sqrt{96\alpha_1^6 - 16\alpha_1^3 + 1} + 1\right)^{1/3}}. \tag{B.1}$$

For higher order moments, the divergence lines are defined by high order algebraic equations, which cannot be solved analytically.

C. Conditions for Γ_4

For a general GARCH conditional probability distribution with variance equal to one, the equation for the sixth-order divergence line (the denominator of equation (10)) becomes:

$$1 - \beta_1^3 - 3\alpha_1\beta_1^2 - 3\eta_4\alpha_1^2\beta_1 - \eta_6\alpha_1^3 = 0. \tag{C.1}$$

Expanding β_1 in a series with respect to α_1 we derive:

$$\beta_1 = 1 - A\alpha_1 - B\alpha_1^2 - C\alpha_1^3 - \cdots. \tag{C.2}$$

Substituting this into our sixth-order divergence line we can equate coefficients up to the second order and so β_1 becomes:

$$\beta_1 = 1 - \alpha_1 - (\eta_4 + 1)\alpha_1^2 + O\left(\alpha_1^3\right). \tag{C.3}$$

If we now neglect α_1 orders higher than the second, we get the equation; $\beta_1 = 1 - \alpha_1 - (\eta_4 + 1)\alpha_1^2$. Substituting this into our equation for the fourth-order standardised moment, we obtain:

$$\Gamma_4 = \frac{\eta_4\left(1 - \alpha_1 - \left(1 - \alpha_1 - (\eta_4 + 1)\alpha_1^2\right)\right)}{1 - \eta_4\alpha_1^2 - 2\alpha_1\left(1 - \alpha_1 - (\eta_4 + 1)\alpha_1^2\right) - \left(1 - \alpha_1 - (\eta_4 + 1)\alpha_1^2\right)^2}. \tag{C.4}$$

Considering the limit when $\alpha_1 \longrightarrow 1$ we finally obtain:

$$\lim_{\alpha_1 \longrightarrow 1} \Gamma_4 = 2\eta_4. \tag{C.5}$$

D. Relations between the Parameters of the Double Gaussian Distribution and Its Higher Order Moments

The normalisation condition for the double Gaussian distribution described by equation (17) is $a + b = 1$. Substituting $a = 1 - b$ into equation (19), $E[x^2]$, we get:

$$b = \frac{1 - \sigma_1^2}{\sigma_2^2 - \sigma_1^2}, \qquad a = \frac{\sigma_2^2 - 1}{\sigma_2^2 - \sigma_1^2}. \tag{D.1}$$

Assuming $\sigma_1^2 < 1 < \sigma_2^2$, and substituting the equations for a and b into the fourth and sixth moment equations we derive:

$$\mu_4 = \sigma_2^2 + \sigma_1^2 - \sigma_1^2\sigma_2^2, \qquad \mu_6 = \left(\sigma_1^2 + \sigma_2^2\right)^2 - \sigma_1^2\sigma_2^2 - \sigma_1^2\sigma_2^2\left(\sigma_1^2 + \sigma_2^2\right) \tag{D.2}$$

where $\mu_4 = \eta_4/3$ and $\mu_6 = \eta_6/15$. Introducing the new variables, $X = \sigma_2^2 + \sigma_1^2$ and $Y = \sigma_1^2\sigma_2^2$, we can simplify the obtained equations:

$$Y = X - \mu_4, \qquad X\left(\mu_4 - 1\right) + \mu_4 = \mu_6. \tag{D.3}$$

Solving the above equations for X and Y we finally obtain:

$$X = \frac{\mu_6 - \mu_4}{\mu_4 - 1}, \qquad Y = \frac{\mu_6 - \mu_4^2}{\mu_4 - 1}. \tag{D.4}$$

Since X and Y must be positive, this gives us three conditions; $\mu_4 > 1$, $\mu_6 > \mu_4$ and $\mu_6 > \mu_4^2$. Due to the first condition, we can disregard the second as $\mu_4^2 > \mu_4$. Using relations between μ_6 and μ_4 and η_4 and η_6 we obtain:

$$\eta_4 > 3, \tag{D.6}$$

$$\eta_6 > \frac{15}{9}\eta_4^2. \tag{D.7}$$

We can then set-up equations for solving σ_1^2 or σ_2^2:

$$\sigma_2^4 - X\sigma_2^2 + Y = 0, \qquad \sigma_1^2 = \frac{Y}{\sigma_2^2}. \tag{D.8}$$

Solving for σ_2^2, we can obtain relations for the parameters of the double Gaussian distribution:

$$\sigma_2^2 = \frac{1}{2}\left(X + \sqrt{X^2 - 4Y}\right). \tag{D.9}$$

And so,

$$\sigma_1^2 = \frac{2Y}{\left(X + \sqrt{X^2 - 4Y}\right)}. \tag{D.10}$$

Since, σ_1^2 and σ_2^2 must be both real and positive, this gives us the relation: $X > 4Y$. As such we get the following inequality:

$$\mu_6^2 - 6\mu_4\mu_6 - 4\mu_6 - \mu_4^2\left(3 - 4\mu_4\right) > 0. \tag{D.11}$$

Solving this inequality for μ_6, we get the condition: $\mu_4 > -1$. Obviously, μ_4 is always larger than -1, and so we always satisfy the condition shown in equation (D.11). As such, the parameters η_4 and η_6 have to only obey the conditions shown in equations (D.6) and (D.7).

E. Quarterly Time-Series Analysis

In this appendix, we show the time evolution for the sixth-order standardised moment for Lloyds Bank and the S&P 500 index, when we truncate the data in quarterly time periods (around 63 days). In Figure 15, it can be seen that compared with the analysis undertaken for the truncation of the sixth-month time period, the quarterly truncation causes very noisy signals. As such, we cannot discern any shared behaviour around any moment in time, particularly not the financial crash of 2008.

We present these findings as an illustrative exercise, taking such a short time window can cause the statistics of these periods to be inaccurate. If we are to assume a Gaussian distribution for the error of these statistics, then the standard error of the metrics scale is $1/n$, where n is the length of time window we take, [34]. Given the sixth- month window is over 100 days, the error for this window is below one percent; however, when we take a window of half of this length, we double our error [30]. Therefore, the conclusions

reached by the analysis of quarterly time periods should be studied with caution.

Data Availability

The authors wish to note the data that support the findings of this study are openly available for all empirical data from https://www.investing.com. Where it was possible, the data have been taken from the London Stock Exchange. The code is available upon request.

Conflicts of Interest

The authors declare that they have no conflicts of interest.

Acknowledgments

The authors would like to thank Professor Alistair Milne for his guidance and advice on this work. A preprint has previously been published [35]. The funding for the research was provided as part of the employment of the authors by Loughborough University.

References

[1] R. F. Engle, "Autoregressive conditional heteroscedasticity with estimates of the variance of United Kingdom inflation," *Econometrica*, vol. 50, no. 4, pp. 987–1007, 1982.

[2] T. Bollerslev, "Generalized autoregressive conditional heteroskedasticity," *Journal of Econometrics*, vol. 31, no. 3, pp. 307–327, 1986.

[3] U. Kumar and K. De Ridder, "Garch modelling in association with fft-arima to forecast ozone episodes," *Atmospheric Environment*, vol. 44, no. 34, pp. 4252–4265, 2010.

[4] G. Ali, "Egarch, gjr-garch, tgarch, avgarch, ngarch, igarch and apgarch models for pathogens at marine recreational sites," *Journal of Statistical and Econometric Methods*, vol. 2, no. 3, pp. 57–73, 2013.

[5] Z. Ding, C. W. J. Granger, and R. F. Engle, "A long memory property of stock market returns and a new model," *Journal of Empirical Finance*, vol. 1, no. 1, pp. 83–106, 1993.

[6] L. Glosten, R. Jagannathan, and D. Runkle, "On the relation between the expected value and the volatility of the nominal excess return on stocks," *The Journal of Finance*, vol. 48, no. 5, 1993.

[7] J. Duan, G. Gauthier, J. Simonato, and C. Sasseville, "Approximating the gjr-garch and egarch option pricing models analytically," *Journal of Computational Finance*, vol. 9, no. 3, 2006.

[8] T. G. Bali and P. Theodossiou, "A conditional-SGT-VaR approach with alternative GARCH models," *Annals of Operations Research*, vol. 151, no. 1, pp. 241–267, 2006.

[9] D. B. Nelson, "Conditional heteroskedasticity in asset returns: a new approach," *Econometrica*, vol. 59, no. 2, pp. 347–370, 1991.

[10] P. R. Hansen and Z. Huang, "Exponential GARCH modeling with realized measures of volatility," *Journal of Business & Economic Statistics*, vol. 34, no. 2, pp. 269–287, 2016.

[11] O. Barndorff-Nielsen, P. Hansen, A. Lunde, and N. Shephard, "Designing realised kernels to measure the ex-post variation of equity prices in the presence of noise," *Econometrica*, vol. 76, no. 6, 2008.

[12] C. Conrad and B. Haag, "Inequality constraints in the fractionally integrated GARCH model," *Journal of Financial Econometrics*, vol. 4, no. 3, pp. 413–449, 2006.

[13] R. Baille, T. Bollerslev, and H. Mikkelsen, "Fractionally integrated generalised autoregressive heteroskedasticity," *Journal of Econometrics*, vol. 74, no. 1, pp. 3–30, 1996.

[14] R. Baille, A. Cecen, and Y. Han, "High frequency deutsche mark-us dollar returns: figarch representations and non linearities," *Multinational Finance Journal*, vol. 4, no. 3-4, pp. 247–267, 2004.

[15] J. M. Woodridge, "Applications of generalized method of moments estimation," *The Journal of Economic Perspectives*, vol. 15, no. 4, pp. 87–100, 2001.

[16] A. R. Hall, *Generalised Method of Moments*, Oxford University Press, Oxford, UK, 2005.

[17] R. Mantegna and H. Stanley, *An Introduction to Econophysics*, Cambridge Press, Cambridge, UK, 2000.

[18] C. Gardiner, *Stochastic Methods*, Springer, Berlin, Germany, 2009.

[19] W. Xu, C. Wu, and H. Li, "Accounting for the impact of higher order moments in foreign equity option pricing model," *Economic Modelling*, vol. 28, no. 4, pp. 1726–1729, 2011.

[20] G. Perez-Quiros and A. Timmermann, "Business cycle asymmetries in stock returns: evidence from higher order moments and conditional densities," *Journal of Econometrics*, vol. 103, no. 1-2, pp. 259–306, 2001.

[21] S.-M. Liu and B. W. Brorsen, "Maximum likelihood estimation of a garch-stable model," *Journal of Applied Econometrics*, vol. 10, no. 3, pp. 273–285, 1995.

[22] L. P. Hansen, "Large sample properties of generalized method of moments estimators," *Econometrica*, vol. 50, no. 4, pp. 1029–1054, 1982.

[23] C. Francq and J.-M. Zakoian, "Quasi-maximum likelihood estimation in GARCH processes when some coefficients are equal to zero," *Stochastic Processes and Their Applications*, vol. 117, no. 9, pp. 1265–1284, 2007.

[24] H. Xuan, L. Song, M. Amin, and Y. Shi, "Quasi-maximum likelihood estimator of Laplace (1, 1) for GARCH models," *Open Mathematics*, vol. 15, no. 1, pp. 1539–1548, 2017.

[25] T. Economist, "Crash course," 2013, https://www.economist.com/schools-brief/2013/09/07/crash-course.

[26] F. C. Drost and B. J. M. Werker, "Closing the GARCH gap: continuous time GARCH modeling," *Journal of Econometrics*, vol. 74, no. 1, pp. 31–57, 1996.

[27] A. Constantinides and S. Savel'ev, "Modelling price dynamics: a hybrid truncated levy-flight garch approach," *Physica A*, vol. 392, no. 9, pp. 2072–2078, 2013.

[28] R. Baille and T. Bollerslev, "Conditional forecast densities from dynamical models with garch innovations," *Journal of Econometrics*, vol. 52, no. 1-2, pp. 91–113, 1992.

[29] K. A. Pokhilchuk and S. E. Savel'ev, "On the choice of garch parameters for efficient modelling of real stock price dynamics," *Physica A: Statistical Mechanics and Its Applications*, vol. 448, no. 15, pp. 248–253, 2016.

[30] L. De-Clerk and S. Savel'ev, "An investigation of higher order moments of empirical financial data and their implications to risk," *Heliyon*, vol. 8, no. 2, 2022.

[31] K. Wallis, "The two-piece normal, binormal, or double Gaussian distribution: its origin and rediscoveries," *Statistical Science*, vol. 29, no. 1, pp. 106–112, 2014.

[32] M. Haas, J. Krause, M. S. Paolella, and S. C. Steude, "Time-varying mixture GARCH models and asymmetric volatility,"

The North American Journal of Economics and Finance, vol. 26, pp. 602–623, 2013.

[33] C. Alexander and E. Lazar, "Normal mixture garch (1,1): applications to exchange rate modelling," *Journal of Applied Econometrics*, vol. 21, no. 3, pp. 307–336, 2006.

[34] B. Everitt and A. Skrondal, *The Cambridge Dictionary of Statistics*, Cambridge University Press, Cambridge, UK, 4th edition, 2010.

[35] L. De-Clerk and S. Savel'ev, *Non-stationary Generalised Autoregressive Conditional Heteroskedasticity Modelling for Fitting Higher Order Moments of Financial Series within Moving Time Windows*, Loughborough University, Leicestershire, UK, 2021.